PROCEEDINGS, 42nd Workshop on Geothermal Reservoir Engineering
Stanford University, Stanford, California, February 13-15, 2017
SGP-TR-212

Hydraulic Fracturing Experiments at 1500 m Depth in a Deep Mine:

Highlights from the kISMET Project

Oldenburg, C.M.[1], Dobson, P.F.[1], Wu, Y.[1], Cook, P.J.[1], Kneafsey, T.J.[1], Nakagawa, S.[1], Ulrich, C.[1], Siler, D.L.[1†], Guglielmi, Y.[1], Ajo-Franklin, J.[1], Rutqvist, J.[1], Daley, T.M.[1], Birkholzer, J.T.[1], Wang, H.F.[2], Lord, N.E.[2], Haimson, B.C.[3], Sone, H.[3], Vigiliante, P.[3], Roggenthen, W.M.[4], Doe, T.W.[5], Lee, M.Y.[6], Ingraham, M.[6], Huang, H.[7], Mattson, E.D.[7], Zhou, J.[7], Johnson, T.J.[8], Zoback, M.D.[9], Morris, J.P.[10], White, J.A.[11], Johnson, P.A.[12], Coblentz, D.D.[13], and Heise, J.[14]

[1]Energy Geosciences Division, Lawrence Berkeley National Laboratory
[2]Department of Geoscience, University of Wisconsin-Madison
[3]Geological Engineering, University of Wisconsin
[4]Geology and Geological Engineering, South Dakota School of Mines & Technology
[5]FracMan Technology Group, Golder Associates Inc.
[6]Sandia National Laboratories
[7]Idaho National Laboratory
[8]Energy and Environment Directorate, Pacific Northwest National Laboratory
[9]School of Earth, Energy, and Environmental Sciences, Stanford University
[10]Atmospheric, Earth, and Energy Division, Lawrence Livermore National Laboratory
[11]Lawrence Livermore National Laboratory
[12]EES-17, Geophysics Group, Los Alamos National Laboratory
[13]Earth and Environmental Sciences Division, Los Alamos National Laboratory
[14]Sanford Underground Research Facility

[†] Now at U.S. Geological Survey, Menlo Park, CA

Keywords: EGS, stress, deep mine, hydraulic fracturing, fractures

ABSTRACT

In support of the U.S. DOE SubTER Crosscut initiative, we established a field test facility in a deep mine and designed and carried out in situ hydraulic fracturing experiments relevant to enhanced geothermal systems (EGS) in crystalline rock to characterize the stress field, understand the effects of rock fabric on fracturing, and gain experience in monitoring using geophysical methods. The project also included pre- and post-fracturing simulation and analysis, and laboratory measurements and experiments. The kISMET (permeability (k) and Induced Seismicity Management for Energy Technologies) site was established in the West Access Drift of the Sanford Underground Research Facility (SURF) 4757 ft (1450 m) below ground (on the 4850 ft level (4850L)) in phyllite of the Precambrian Poorman Formation. We drilled and continuously cored five near-vertical boreholes in a line on 3 m (10 ft) spacing, deviating the two outermost boreholes slightly to create a five-spot pattern around the test borehole centered in the test volume 40 m below the drift invert (floor) at a total depth of ~1490 m (4890 ft). Laboratory measurements of core from the center test borehole showed P-wave velocity heterogeneity along each core indicating strong, fine-scale (~1 cm or smaller) changes in the mechanical properties of the rock. Field measurements of the stress field by hydraulic fracturing showed that the minimum horizontal stress at the kISMET site averages 21.7 MPa (3146 psi) trending approximately N-S (356 degrees azimuth) and plunging slightly NNW at 12°. The vertical and horizontal maximum stresses are similar in magnitude at 42-44 MPa (6090-6380 psi) for the depths of testing, which averaged approximately 1530 m (5030 ft). Hydraulic fractures were remarkably uniform suggesting core-scale and larger rock fabric did not play a role in controlling fracture orientation. Analytical solutions suggest that the fracture radius of the large fracture (stimulation test) was more than 6 m (20 ft), depending on the unknown amount of leak-off.

1. INTRODUCTION

The design and execution of effective fracture creation and fracture stimulation for enhanced geothermal systems (EGS) depend on knowledge of key properties such as stress state, rock structure and fabric, existing fractures, and permeability. The difficulty of characterizing these properties before and after stimulation in the deep subsurface results in incomplete knowledge of the effects of active fracturing and stimulation, thereby preventing development of advanced adaptive control of fractures for permeability management, a major goal of the U.S. DOE SubTER Crosscut initiative. Similarly, remote monitoring of microseismicity associated with fracturing and stimulation can result in uncertain event locations and low-resolution mapping of fracturing processes. Deep mine environments offer the possibility of detailed characterization and proximal monitoring of intermediate-scale hydraulic fracturing and fracture stimulation, which in turn provide high-resolution data sets for improved understanding of stimulation and related modeling and simulation developments and testing.

Oldenburg, Dobson, and the entire kISMET team

In order to address the challenges of subsurface energy-related processes involving fractures, fracturing, and permeability enhancement, earth scientists from several national laboratories and three universities have carried out a $1.35M project to develop a new underground facility called kISMET (permeability (k) and Induced Seismicity Management for Energy Technologies) located 4757 ft (1450 m) below ground at the Sanford Underground Research Facility (SURF) in Lead, South Dakota. The purpose of the new facility is to provide a test site for research on stress characterization, permeability enhancement, and induced seismicity in crystalline rock. Rocks at SURF comprise a sequence of intensely folded Precambrian metamorphic schists, phyllites, and amphibolites cut by a number of Tertiary rhyolite dikes.

Following site selection in the spring of 2015 based on satisfying multiple practical and scientific criteria, we designed a borehole array for the West Access Drift on the 4850L (nominally 4850 ft below ground) and drilled and cored five approximately vertical boreholes on 3 m (10 ft) spacing: one center NQ borehole 100 m (328 ft) deep, and four surrounding HQ boreholes 50 m (164 ft) deep. The four monitoring boreholes were instrumented with active seismic and electrical resistivity monitoring equipment, and accelerometers were placed in the 4850L drift for measuring induced microseismicity.

Starting in August 2016, we carried out hydraulic fracturing-based stress measurements and stimulation that determined the stress field. In parallel, laboratory studies on core from the boreholes were initiated to measure key rock properties. Following the field testing, analytical solutions were applied using field data to estimate the sizes of fractures generated. Here, we present some highlights of activities and findings of the kISMET project. Details and additional information can be found in the summary report (Oldenburg et al., 2016).

2. SITE-SELECTION, CHARACTERIZATION, AND INFRASTRUCTURE

Several criteria were used to locate the kISMET site, among which were preference for a single lithology and simple structure to avoid excessive heterogeneity and complexity, availability of key services such as ventilation, power, internet, and sufficient room for drilling and testing activities without impeding access in the drift for SURF operations. We also required a site at sufficient depth (thickness of overburden) to provide stress conditions representative of deep EGS sites, and we wanted to avoid local stress perturbations caused by drifts immediately above, below, or astride the site. Figure 1 shows the location of SURF and the chosen kISMET site in the West Access Drift on the 4850L in Poorman Formation phyllite with no other drifts nearby.

(a)

(b)

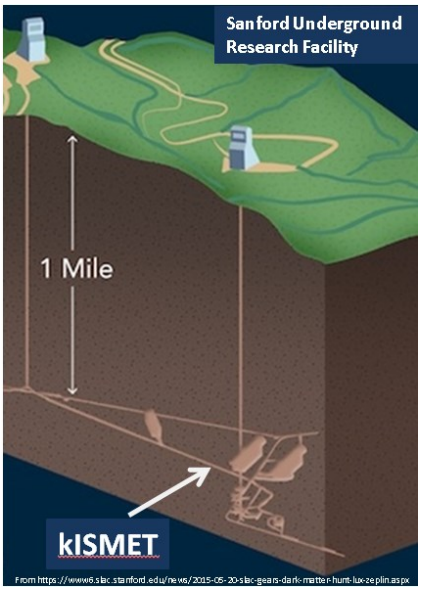

Figure 1: Location map showing (a) SURF in Lead, SD, and (b) the location of the kISMET site on the 4850L putting the site at 4757 ft (1450 m) below ground surface.

We designed a five-borehole array as shown in Fig. 2a consisting of four monitoring boreholes surrounding a central injection borehole in which stress measurements and stimulation were carried out. A vertical orientation for the test borehole was chosen so it would align approximately with the σ_1 principal stress direction, which at this depth, 4757 ft (~1450 m), is approximately vertical ($\sigma_1 = \sigma_v$) due to overburden stress. We developed a drilling design in which the five borehole collars are aligned in the drift with the outer-most boreholes drilled slightly deviated such that the four monitoring boreholes and central test borehole would form a five-spot configuration around a test volume at a completion depth of 50 m (164 ft). We decided to drill the central experimental borehole even deeper (100 m, or 328 ft) in order to provide space at depth to conduct the first stress measurements and test the equipment, thus reserving the shallower parts of the borehole to conduct the monitored fracturing experiments including the extended fracture test, also called the stimulation test. Borehole spacing was chosen on the basis of the desire for proximal monitoring of the initiation and growth of the hydraulic fractures, while not having the boreholes so close that the fractures would grow far beyond the monitoring boreholes of

the test volume. The final decision was on borehole diameter with considerations including size of cores to be collected, flexibility in deploying existing monitoring and fracturing equipment rather than buying all new equipment, and ease of controlling the drilling in this foliated phyllite. Our final design called for four HQ (dia. = 3.78 inches, 96 mm) monitoring boreholes 50 m (164 ft) deep on 3 m (9.8 ft) spacing, and a central NQ (dia. = 2.98 inches, 75.7 mm) borehole, which was drilled to 100 m (328 ft) depth to provide extra test length for stress measurements and equipment shakedown.

(a)

(b)

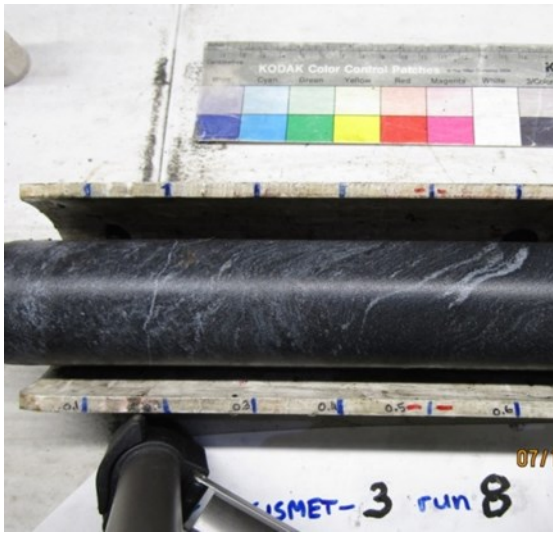

Figure 2: (a) Borehole array showing the five borehole collars aligned in the 4850L drift, with outer-most boreholes deviated to create a five-spot pattern at 164 ft (50 m) below the drift. Although not shown, the center borehole extends approximately vertically to 330 ft (100 m) below the drift. The inner two boreholes are vertical and extend to 164 ft (50 m). (b) Example photograph of phyllite cored from borehole kISMET-003, core run 8 (units in tenths of feet).

The SURF support group installed rock bolts and safety mesh, electrical power, internet, sump, fresh water supply, and access to a water disposal line, and provided escort and logistical support for equipment transport from surface to the kISMET site. The drilling crew began mobilizing at Lead, SD, on June 13, 2016, and finished drilling and coring the final borehole on July 20, 2016. During drilling, intermediate gyro surveys were made to monitor the orientation of the boreholes, and a final survey was made at the bottom-hole locations at the end of drilling. There was 100% recovery of core, which consisted of banded and often tightly folded but unfractured phyllite of the Poorman Formation as shown in Figure 2b. Only one small open fracture was observed in the core. Each section of core was described and photographed at the site, and then stored in core boxes, which were transported to the surface for storage at the SURF core repository.

Borehole deviation was measured twice after drilling and coring were completed, once using a dedicated borehole deviation tool, and a second time using the integrated deviation sensors on the optical televiewer. The magnetic deviation data showed a maximum of ~6.5 m (21.3 ft) XY deviation relative to surface locations for the two outermost deviated boreholes (kISMET-001 and kISMET-005). The two inner vertical monitoring boreholes were shown to deviate less than 0.8 m (2.6 ft) from vertical. While the bottom of the central test borehole (kISMET-003) deviated roughly 6 m (19.7 ft) from vertical at 100 m depth, the top 50 m of the borehole deviated only ~2 m (6.6 ft) from the vertical direction, creating a nominal five-spot pattern around the test volume at 40 m (131 ft) depth.

3. LABORATORY MEASUREMENTS ON CORE

Laboratory core studies aimed (1) to characterize the mechanical and hydrological properties of the Poorman phyllite and (2) to examine the impact of the rock fabric and in situ stress anisotropy on hydraulic fracturing. The rock samples used in the laboratory experiments were obtained from core from the central test borehole, kISMET-003. For baseline rock property characterization tests, we used X-ray CT imaging and ultrasonic velocity measurements, followed by measurements of tensile strength and flow permeability. CT scans of core show well-developed laminations that are tightly folded; heterogeneity in rock fabric occurs even at the centimeter scale.

P-wave velocity was measured using a pair of narrow-band immersion transducers for a range of orientations and locations along the cores. For each core, the reference orientation was determined from the texture (foliation) on the surface of the cores. Cores exhibited very strong velocity anisotropy (as much as 15%) and a well-defined peak orientation, possibly resulting from rock foliation. Velocity changes (heterogeneity) along each core indicate strong, fine-scale (~1 cm or smaller) changes in the mechanical properties of the rock, possibly due to the well-developed foliation.

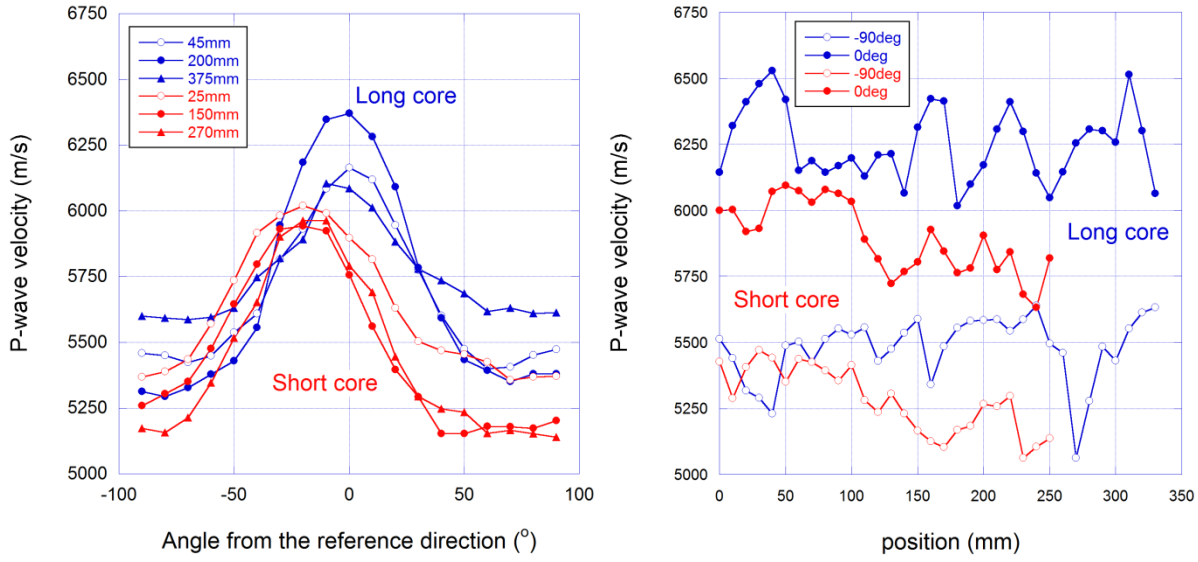

(a) Velocity anisotropy (b) Velocity heterogeneity

Figure 3. Seismic P-wave velocity anisotropy around (a) and along (b) the two cores. Very clear anisotropy is present for the entire lengths of the cores. Velocity also varies rapidly along the cores, possibly because of sub-centimeter-scale laminae with strong contrasts in elastic moduli. Note that the anisotropy is characterized only within planes perpendicular to the core axis. The smallest P-wave velocity in the rock can be even smaller in the direction perpendicular to the mean foliation planes.

Short disc-shaped samples of the core (dia. = 25.4 mm, thickness= ~10–13 mm) were used for Brazilian disc tests. The objective of these measurements is to understand the impact of the foliation plane on the tensile strength, crack formation, and crack propagation behavior in the rock. The sample plugs have their plug-cylinder axis parallel to the foliation. The load-displacement record suggests that the elastic stiffness is anisotropic, especially in samples from core where the rock appears stiffest when loaded parallel to the foliation, consistent with the velocity measurements. Tensile strength is also strongly anisotropic for sample types where the rock is easier to split when loaded parallel to the foliation. Tensile strength ranges between 3–7.5 MPa and 5–12 MPa. The foliation, mostly defined by the alignment of phyllosilicate minerals, serves as a weak plane and seems to have influenced the fracture path of samples loaded diagonally relative to the foliation. Samples are planned to be scanned by X-ray CT imaging in order to characterize the morphology of the fractures created in these tests. See Oldenburg et al. (2016) for more information.

4. STRESS MEASUREMENT AND STIMULATION

The main purpose of the kISMET project was to carry out hydraulic fracturing experiments at depths of approximately 5000 ft (1500 m) for determining the in situ stress field, for testing the creation of a larger fracture (stimulation), and for observing the effects of rock fabric on fracturing while monitoring the process using various geophysical approaches. Motivation for new measurements of the stress field at SURF arose from a long history of highly variable stress measurements, for which the source of variability was not well known and could be due to rock heterogeneity, anisotropy, or shortcomings of measurement techniques. In order to meet the SubTER goal of developing approaches to control fracturing at depth, further understanding is needed of the effects of rock fabric, the stress field, and hydraulic fracturing processes.

Characterization of the stress field at SURF began in the 1970's, when the site was an active gold mine, and continued ever since for satisfying the stress characterization needs for new mining excavations, and later for DUSEL and SURF cavern designs. A compilation of measurements with wide scatter was regressed to derive approximate equations for σ_v, σ_{HMax}, and σ_{Hmin} as a linear function of depth. The ratio of maximum-horizontal-to-vertical stress is between 0.6 and 0.9 and the ratio of minimum horizontal stress to vertical stress is between 0.36 and 0.6 (Pariseau, 1986). More recent measurements provided stress values that ranged from close to 62 MPa (9000 psi) to 24 MPa (3500 psi) for the largest and smallest stresses, respectively, and were highly variable in both direction and magnitude depending on location and rock type at SURF (Golder Associates, 2010).

Hydraulic fracturing has become a standard method for determining the in situ state of stress in rock masses for use in engineering design, and is one of the few methods available for testing in deep boreholes (Haimson, 1978). Although numerous past measurements of in situ stress have been made at SURF over the years, the present measurements are the first to be performed using hydraulic fracturing. The technology we used at kISMET utilizes a fast and continuous tool-tripping wireline hydraulic fracturing system for in situ stress measurements and fracture stimulation. The wireline hydraulic fracturing system we used consists of a straddle packer assembly for fracture initiation and propagation (stimulation) within the selected test zone as shown in Figure 4. We used an acoustic televiewer for fracture delineation following fracturing. In order to run hydraulic fracturing tests, hydraulic fluid pressure is generated by two pneumatic pumps (one for the packers and the other for the test zone between the packers). A flow meter is also employed to

monitor the flow of water into (and out of) the test zone during (de) pressurization. The flow rate of the injection fluid into the fracturing test zone is monitored by a turbine flowmeter connected between the surface pump and the high-pressure tubing leading to the test zone. The packer and test-zone pressures as well as the flow rate are recorded simultaneously on a portable computer at 10 samples/s to allow statistical analysis for determining shut-in and fracture reopening pressures.

(a)

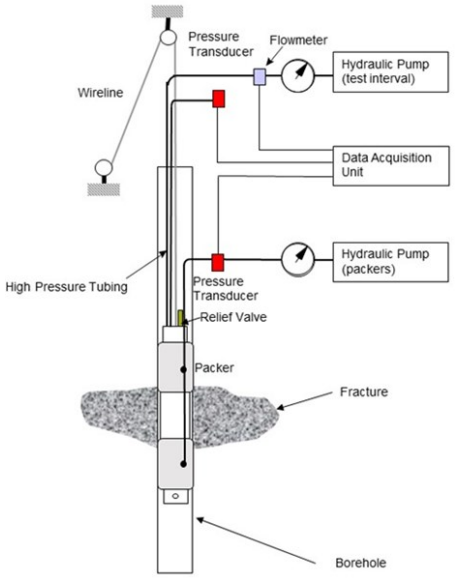

(b)

Figure 4: (a) Wireline straddle-packer hydraulic fracturing system. (b) Pressure generators and digital data recorders used for hydraulic fracturing and fracture stimulation at SURF.

To perform a hydraulic fracturing stress measurement, a section of a borehole is hydraulically isolated using the flow rate-straddle packer assembly while fracturing fluid (water) is pumped at a low flowrate into the packed-off interval, gradually raising the pressure on the borehole wall until a fracture is initiated in the rock, indicated by a drop of the fluid pressure. Pumping is stopped allowing the test interval pressure to decay. Several minutes into the shut-in phase, the pressure is released and allowed to return to ambient conditions. The pressure cycle is repeated three times maintaining a similar flowrate. The key measures of breakdown, re-opening, and shut-in pressures are picked from the pressure–time record and used in the computation of the in situ stress.

We tested intervals above 72 m (236 ft) in depth including the stimulation test zone at 40.2 m (1490 m below ground surface). Test data quality was excellent with well-defined breakdown pressures and clear shut-in pressure signatures as shown in Figure 5 as an example. Our measured minimum horizontal stress (σ_{Hmin}) values range from 20.0 to 24.1 MPa, averaging 21.7 MPa (3146 psi), approximately 51% of the estimated lithostatic stress. The values have a high level of consistency that is typical for hydraulic fracturing stress measurements in low-permeability, relatively uniform rock. The stimulation test involved keeping the generated fracture open and propagating during a period of constant pressure and low flow rate. Following initiation of the hydraulic fracture as indicated by breakdown at 22.7 MPa (3291 psi), five stimulation cycles were conducted. The first two cycles were conducted with a relatively low flow rate of 0.48 lpm, while the next three cycles used a relatively high flowrate of 0.63 lpm. For each cycle, the steady-state pressures were achieved at 20.1-20.3 MPa (2914-2943 psi) and maintained for approximately 15 minutes in order to finish one round of electrical resistivity tomography (ERT) data acquisition; continuous active source seismic monitoring (CASSM) acquisition takes only ~20 sec.

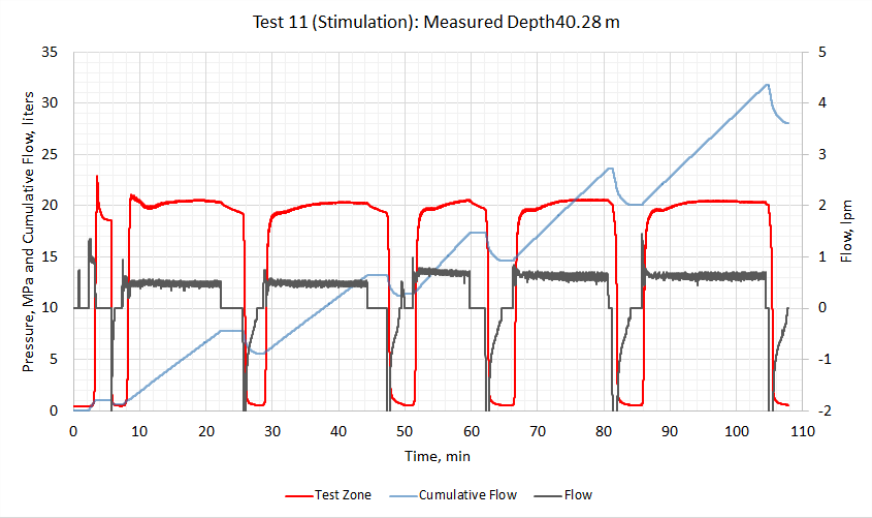

Figure 5: Pressure, flow, and cumulative flow for the kISMET stimulation test.

Maximum horizontal stress (σ_{Hmax}) can be estimated if rock tensile strength is known, measurements of which are ongoing in the lab. Maximum horizontal stress can also be estimated from the difference between the breakdown pressure P_b achieved in the first pressure cycle, and the fracture reopening pressure Pr recorded in the second pressure cycle using the method of Haimson and Cornet (2003). The maximum horizontal stress values estimated in this way range from 38.7 to 48.2 MPa with an average of 44.1 MPa (6394 psi), close to the lithostatic stress. While there is uncertainty in this estimate of σ_{Hmax}, it appears that at this depth, the vertical stress and maximum horizontal stresses are similar in magnitude which may be indicative of the cross-over from a tendency for strike-slip faulting at shallow crustal depths to a tendency for normal faulting at greater depth (Zoback et al., 2003).

As for the stress directions, fractures created by hydraulic fracturing in homogeneous rock should align with the direction of the maximum horizontal stress (σ_{Hmax}). We obtained fracture orientation information from the acoustic televiewer log as shown in Figure 6. The analysis of the acoustic televiewer logs involved digitizing the fracture traces and importing them to an Excel spreadsheet, where they were fitted to sinusoidal traces of known orientation. The quality and consistency of the fracture orientations mirror that of the shut-in pressures from the hydraulic fracturing. Overall the data set provides an excellent indicator of the minimum horizontal stress (σ_{Hmin}) direction with a 356° trend and 12° plunge indicating fractures that are striking N86°E with a dip of 78° to the southeast. The fact that the fractures are not following foliation but have a non-vertical, though very steep, dip indicates that the principal stress may be inclined slightly off vertical. The uniformity of results as shown in Figure 7 across tens of meters of depth in the test borehole suggests that stress rather than rock fabric is controlling hydraulic fracture orientations. Reviews of midcontinent stress measurements suggest a relatively uniform compressive stress field with a maximum horizontal stress (σ_{HMax}) oriented NE to ENE (Zoback and Zoback, 1989). Our measurements at kISMET are consistent with this general direction of the regional horizontal principal stresses (σ_{HMax} trending NE to ENE). The kISMET determination of average principal stress magnitudes of $\sigma Hmax \approx \sigma v \approx 2\sigma_{Hmin}$ is also in accord with the regional conditions.

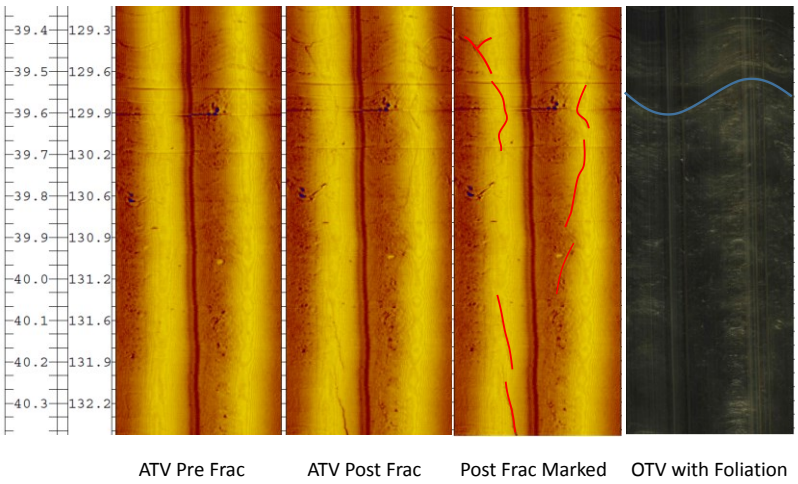

Figure 6: Acoustic televiewer logs for the Test 11 stimulation zone (40.23 m depth in borehole).

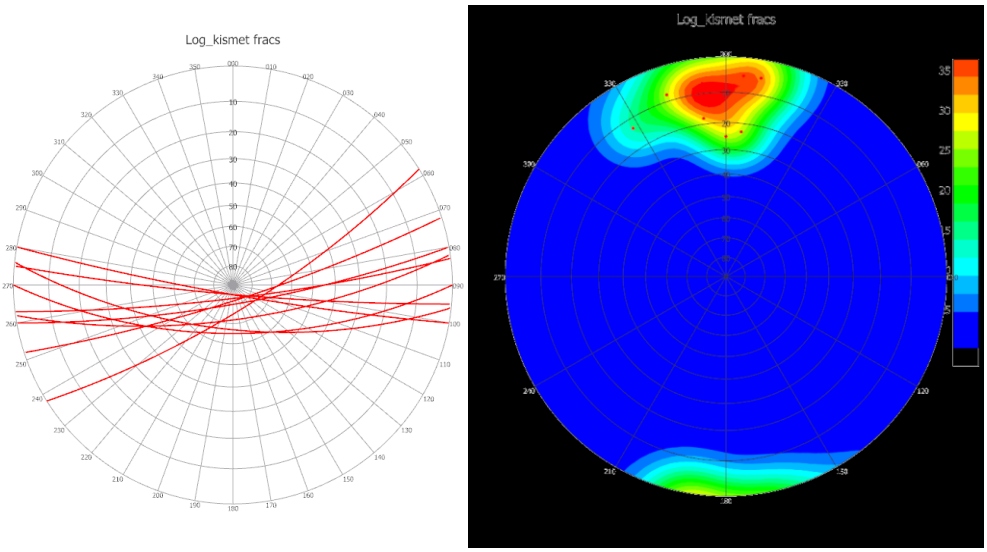

Figure 7: Stereographic projections of hydraulic fractures at the kISMET site. Left: plane plot. Right: contoured pole plot.

5. MODELING AND SIMULATION

An important part of the kISMET experimental design was the determination of the injection parameters (duration of injection at given flow rate) to produce hydraulic fractures with desired size ranges. A second objective of design calculations was to provide an initial conservative estimate of the magnitudes of potential seismicity induced by the hydraulic fracturing experiments under various injection scenarios. We used INL's FALCON coupled network flow and quasi-static discrete element model (DEM) to predict fracture size, breakdown pressure, fracture re-opening pressure, and energy released by fracturing. Results of these simulations are described in the companion paper by Huang et al. (2017) presented concurrently at the Stanford Geothermal Workshop and will not be duplicated here. Instead, we highlight here some estimates of fracture size made using analytical solutions.

The kISMET hydraulic fracturing experiments allowed determination of the magnitude and orientation of the minimum and maximum horizontal stresses (magnitude and orientation) at the kISMET site, but did not provide a direct measurement of fracture size. Takahashi and Abé (1987) provide the essential relationships of fracture radius and aperture to injected fluid volume:

$$R = \sqrt[5]{\left(\frac{Q_e D}{\pi^{3/2} K_{1C}}\right)^2} \tag{1}$$

$$D = \frac{3\pi E}{8\left(1-\nu^2\right)\rho} \tag{2}$$

$$e_{\max} = \frac{4\left(1-\nu^2\right)}{E}\left(\frac{R}{\pi}\right)^{1/2} K_{1C} \tag{3}$$

where e_{max} is the aperture at the borehole wall, R is fracture radius, ν is Poisson's ratio, and ρ is the fluid density. D is a lumped parameter and Q_e is the effective fluid mass injected (total injected mass minus leak off).

Assuming the penny crack conceptual model is appropriate for the hydraulic fracture generated in the kISMET Experiment 11 (stimulation test shown in Figure 5), we have used analytical equations along with available rock property data and data on injection flow rates and volumes to estimate fracture size. Using the field data, which showed a total fluid injection volume of 41.8 liters and total bleed-back over five cycles of -13.8 liters, the net fluid injection volume is 28.1 liters. Assuming no leak-off (zero rock permeability), all of the water goes into fracture creation, i.e., the fluid volume that is creating the fractures is the net volume of injected water minus the bleed back. The analytical equations for this case suggest that the fracture expanded to a radius of 7.9 m (26 ft) through stimulation Cycles 2 to 6, with relatively small radial growth in the last cycle. The equation estimates that fracture aperture values grew from 4.3×10^{-5} m to 8.5×10^{-5} m (0.043 – 0.085 mm). We refer readers to Oldenburg et al. (2016) for discussion of fracture size for the case on non-zero rock permeability, i.e., with leak-off.

Table 1. Fracture radius, area, and aperture calculations for impermeable rock (Eqs. 1-3).

Cycle	Rate	Duration	Net Injected Volume	Radius	Area	Aperture at Borehole	Fracture Propagation Resistance
	lpm	min	liters	m	m^2	m	MPa
Cycle 1	1.2	0.81	1.01	2.0	12.7	4.27E-05	0.62
Cycle 2	0.5	14.90	7.80	4.6	65.4	6.42E-05	0.41
Cycle 3	0.4	17.48	13.20	5.6	99.6	7.14E-05	0.37
Cycle 4	0.7	8.11	17.40	6.3	124.3	7.54E-05	0.35
Cycle 5	0.6	14.42	23.50	7.1	158.1	8.01E-05	0.33
Cycle 6	0.6	17.72	31.20	7.9	198.3	8.48E-05	0.31

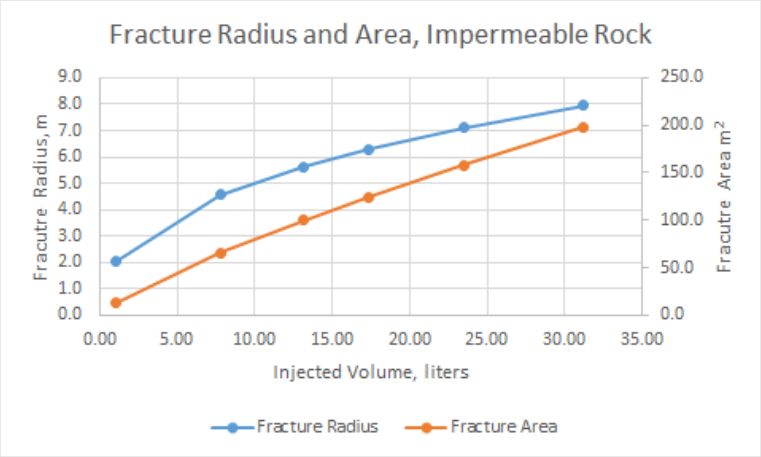

Figure 8: Calculated fracture area and radius for impermeable rock.

6. MONITORING

Borehole logging and geophysical monitoring were conducted before, during, and after hydraulic fracturing stress testing and stimulation at kISMET. Continuous Active Seismic Source Monitoring (CASSM) data have not been analyzed yet. Crosswell ERT surveys were conducted to provide information concerning the geologic structure, fabric, and heterogeneity of the host rock, and to assess the capability of ERT to image the fracturing in near-real time. Two electrode cables with electrode spacing of 1.6 m (5.25 ft) were used to collect crosswell imaging data separately between different well pairs across the kISMET test volume. With electrodes deployed in the K2-K4 well pair, crosswell ERT data sets were collected before and after stimulation operations using a survey configuration designed to optimize both spatial and temporal imaging resolution. With electrodes deployed in the K1-K5 well pair, additional crosswell ERT data sets were collected before, during, and after stimulation operations. Baseline pre-stimulation data were inverted simultaneously in 3D including explicit modeling of boreholes in true dimension and with deviations, along with explicit modeling of borehole fluid conductivity. The baseline images revealed steeply dipping electrical conductivity variations consistent with the host rock structure and mineralogy at the site.

We used a computational mesh for ERT data inversion that accounted for borehole geometry variations. Within the boreholes, the starting model for the inversion was set to the assumed borehole-fluid conductivity, but this starting model fluid conductivity was allowed to be modified by the inversion subject to being smoothly varying within the borehole. Fluid conductivities were allowed to vary because water samples collected from each well and analyzed after the stimulation revealed significantly different fluid conductivity between wells (~500 to > 1000 μS/cm). Time-lapse images from both the K1-K5 and K2-K4 planes were not able to distinguish the induced fracture, likely due to the combined effects of a relatively small fracture zone, changes in borehole fluid conductivity during the imaging campaign, and the geometry of the imaging planes with respect to the fracture zone.

Passive seismic monitoring using accelerometers located on concrete footings in the 4850L drift recorded continuously during hydraulic fracturing activities. Only the deepest hydraulic fracturing tests produced usable signals above background noise. For these tests, the accelerometer recorded the breakdown event and subsequent fracture re-openings. Shallower hydraulic fracturing events did not produce signals discernable above the considerable noise of the pumps at the kISMET site. Future use of passive seismic monitoring should use borehole-based accelerometers to minimize noise from equipment in the drift.

7. CONCLUSIONS

The kISMET team carried out a successful program of drilling and coring, and subsequent hydraulic fracturing for determining the stress field, understanding the effects of rock fabric on fracturing, and gaining experience in monitoring the fracturing process. Laboratory measurements of core show strong effects of anisotropy, and additional laboratory-based permeability measurements are planned, as are two types of laboratory-scale hydraulic fracturing experiments. Pre-fracturing numerical simulation results were in good agreement with analytical estimates and observations. Field measurements of the stress field by hydraulic fracturing showed that the minimum horizontal stress at the kISMET site averages 21.7 MPa (3146 psi) pointing approximately N-S (356 degrees azimuth) and plunging slightly NNW at 12°. Hydraulic fractures were remarkably uniform suggesting core-scale and larger rock fabric did not play a role in controlling fracture orientation. Monitoring using ERT and CASSM in the four monitoring boreholes, and passive seismic accelerometer-based measurements in the West Access Drift, were carried out during the long fracturing (stimulation) test. ERT was not able to detect the fracture created, while the accelerometers in the drift picked up only the fracturing signal from the first (deepest) hydraulic-fracturing stress measurement.

ACKNOWLEDGMENTS

Special thanks to David Vardiman, Tom Regan, Bryce Pietzyk, and other members of the SURF underground field team for help with underground testing and logistical support. We also thank FirstDrilling for safe and efficient drilling (and coring) of the kISMET boreholes. Thanks are also due to Alexandra Prisjatschew and Eric Hass (DOE Geothermal Technologies Office) for project management and encouragement. This work is supported by the SubTER Crosscut Initiative of the U.S. Department of Energy, and by Lawrence Berkeley National Laboratory under US Department of Energy Contract No. DE-AC02-05CH11231.

REFERENCES

Golder Assoc. (2010). In situ Stress Measurement Deep Underground Science and Engineering Laboratory. Prepared for South Dakota School of Mines and Technology, January 8, 2010. Lakewood, CO: Golder.

Haimson, B.C. and Cornet, F.H. (2003). ISRM Suggested Method for Rock Stress Estimation: Hydraulic Fracturing and Hydraulic Testing of Pre-Existing Fractures, Intl. J. Rock Mech. and Mining Sci., 40, 1011-1020.

Zhou, J., et al., (2017) Modeling of Hydraulic Fracture Propagation at the kISMET Site Using a Fully Coupled 3D Network-Flow and Quasi-static Discrete Element Model, Stanford Geothermal Workshop, February 13-15, 2017.

Oldenburg, C.M., P.F. Dobson, and 30 others, Intermediate-Scale Hydraulic Fracturing in a Deep Mine, kISMET Project Summary 2016, Lawrence Berkeley National Laboratory Report, LBNL-1006444, 2016.

Takahashi, H. and Abé, H. (1987). Fracture mechanics applied to hot, dry rock geothermal energy, in B. Atkinson ed, Fracture Mechanics of Rock, Academic Press, p 241-276.

Zoback, M.D., Barton, C.A., Brudy, M., Castillo, D.A., Finkbeiner, T., Grollimund, B.R., Moos, D.B., Peska, P., Ward, C.D., and Wiprut, D.J. (2003). Determination of stress orientation and magnitude in deep wells. International Journal of Rock Mechanics and Mining Sciences, 40(7), pp.1049-1076.

Zoback, M.L. and Zoback, M.D. (1989). Tectonic stress field of the continental United States, Geological Society of America Memoir 172, Chapter 24, 523-540.